A strategy for probing the evolution of crystallization processes by low-temperature solid-state NMR and dynamic nuclear polarization

Paolo Cerreia Vioglio,[†] Pierre Thureau,[†] Marie Juramy,[†] Fabio Ziarelli,[‡] Stephane Viel,[†,¶]

P. Andrew Williams,[§] Colan E. Hughes,[§] Kenneth D. M. Harris*[,§] and Giulia Mollica*[,†]

[†] Aix Marseille Univ., CNRS, ICR, Marseille, France

[§] School of Chemistry, Cardiff University, Park Place, Cardiff, Wales, CF10 3AT, U. K.

[¶] Institut Universitaire de France, Paris, France

[‡] Aix Marseille Univ., CNRS, Centrale Marseille, FSCM, Marseille, France

Corresponding Authors

giulia.mollica@univ-amu.fr; HarrisKDM@cardiff.ac.uk

ORCID Numbers:

KDMH: 0000–0001–7855–8598

GM: 0000–0002–6896–2447

ABSTRACT

Crystallization plays an important role in many areas, and to derive a fundamental understanding of crystallization processes, it is essential to understand the sequence of solid phases produced as a function of time. Here, we introduce a new NMR strategy for studying the time-evolution of crystallization processes, in which the crystallizing system is quenched rapidly to low temperature at specific time points during crystallization. The crystallized phase present within the resultant "frozen solution" may be investigated in detail using a range of sophisticated NMR techniques. The low temperatures involved allow dynamic nuclear polarization (DNP) to be exploited to enhance the signal intensity in the solid-state NMR measurements, which is advantageous for detection and structural characterization of transient forms that are present only in small quantities. This work opens up the prospect of studying the very early stages of crystallization, at which the amount of solid phase present is intrinsically low.

TOC GRAPHIC

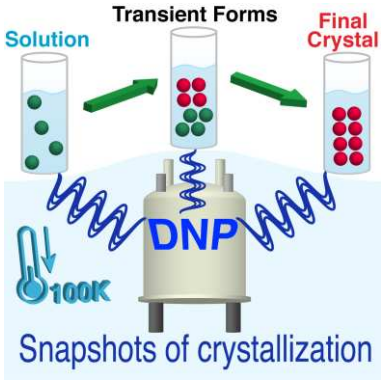

KEYWORDS: Nuclear Magnetic Resonance, Crystallization, Polymorphism, Transient States, Signal Enhancement, Glycine

Crystallization processes are important in many aspects of chemical, pharmaceutical and biological sciences, and are critical in underpinning several industrial applications.[1] In many cases, crystallization evolves through a sequence of intermediate solid forms (e.g., polymorphs, solvates or amorphous phases) before reaching the final thermodynamically stable crystalline phase.[2,3] The intermediate solid forms often have only transient existence, but they nevertheless represent significant stages in the crystallization pathway. Clearly, to derive a comprehensive understanding of crystallization mechanisms, it is essential to know the sequence of solid phases produced as a function of time.[4] The ability to understand the time-evolution of the solid phase is crucial if strategies are to be designed for controlling the formation of a specific desired polymorph or inhibiting the formation of undesirable polymorphs, potentially with huge economic consequences in industrial applications of crystallization.

Several *in-situ* characterization techniques have been developed to monitor the evolution of crystallization processes and to provide insights into fundamental aspects of crystallization.[5, 6] In recent years, there has been increasing interest in the development and application of solid-state NMR strategies for *in-situ* monitoring of crystallization, particularly to establish the sequence of solid phases present as a function of time.[7-14] The time-resolution that can be achieved in *in-situ* solid-state NMR studies of crystallization depends on the time to record an individual spectrum of adequate quality to distinguish the different solid forms present at each stage of the process. However, even to record a simple one-dimensional solid-state NMR spectrum may require several tens of minutes (depending on isotopic abundance, the type of NMR measurement, relaxation times, magnetic field strength, etc), and the use of more sophisticated measurement techniques (e.g., two-dimensional correlation spectra, which yield more detailed structural insights) is generally not viable within the context of *in-situ* solid-state NMR studies of crystallization. Problems due to low sensitivity are particularly exacerbated in studying the earliest stages of crystallization, when the amount of solid phase present is intrinsically low.

In this paper, we report an alternative (*ex-situ*) solid-state NMR strategy to explore the time-evolution of crystallization processes, in which the system is studied at specific time points during crystallization by quenching the system rapidly to low temperature.[15-18] Rapid freezing of the crystallization solution (to *ca.* 100 K) stops the crystallization process and the crystallized phase within the resultant "frozen solution" may then be investigated in detail using a range of NMR techniques, allowing in-depth structural characterization. If new transient solid forms are observed within the frozen solution, such NMR techniques have the potential to reveal detailed insights into their structural properties. Furthermore, the low temperatures involved allow dynamic nuclear polarization (DNP)[19-32] to be exploited to enhance the signal intensity in solid-state NMR studies of the frozen crystallization system.

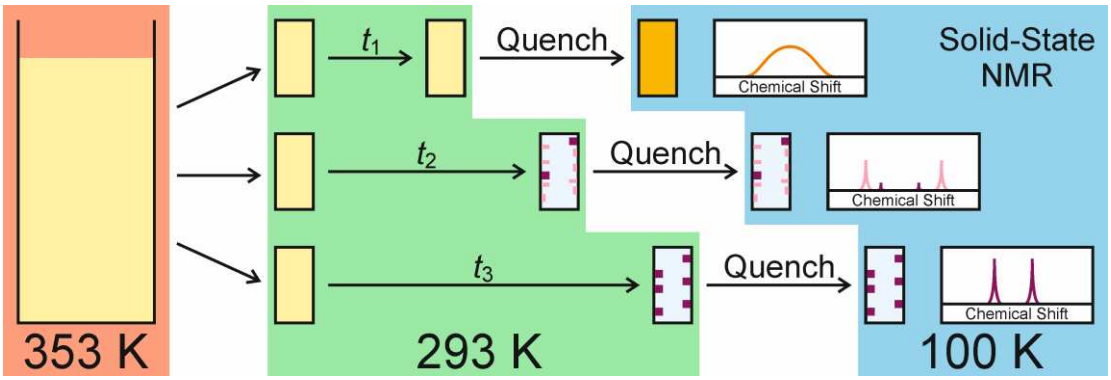

Figure 1. Schematic of the experimental strategy reported here to probe the evolution of crystallization processes

In our strategy (Figure 1), an under-saturated solution is prepared at high temperature and then separated into several identical NMR rotors, which are cooled to ambient temperature to induce crystallization. Crystallization is allowed to proceed in parallel in each rotor under identical conditions at constant temperature. At specific points in time during the crystallization process, one of the rotors is subjected to rapid freezing (to *ca.* 100 K in less than 1 min) inside the NMR spectrometer, followed by measurement of solid-state (DNP) NMR data. The NMR data recorded for each frozen solution effectively represents a snapshot of the solid phase(s) present in the crystallization system at a specific point in time during the crystallization process.

The method is demonstrated here in studies of crystallization of glycine [$H_2C(NH_3^+)(CO_2^-)$], which is widely used as a model polymorphic system in studies of crystallization. Glycine has three known polymorphs (denoted α, β and γ) under ambient conditions.[33-36] The thermodynamically stable form is the γ polymorph and the least stable form is the β polymorph.[37, 38] According to literature, crystallization of glycine from water at neutral pH produces the meta-stable α polymorph, while crystallization of glycine from deuterated water has been reported[35,4, 8, 39] to increase the probability of forming the γ polymorph. The isotropic ^{13}C chemical shifts for the carboxylate carbon in the α, β and γ polymorphs differ by *ca*. 1 ppm,[40] allowing them to be readily distinguished by solid-state ^{13}C NMR. A crystalline dihydrate phase of glycine has also been reported recently.[41, 42]

As a preliminary consideration, we were concerned whether rapid quenching of the crystallization system in our experimental protocol might actually trigger rapid crystallization to occur within the solution phase, which would clearly compromise the interpretation of the NMR data recorded for the frozen crystallization solution. To assess this issue, aqueous solutions of 1-^{13}C-glycine were prepared at concentrations (0.5 M and 1.8 M) that are under-saturated at ambient temperature, and were subjected to rapid quenching (to *ca*. 100 K in less than 1 min) in the NMR spectrometer. The $^{1}H \rightarrow ^{13}C$ CPMAS NMR spectra recorded for these quenched systems (Figure S1 in SI) showed only a broad signal corresponding to an amorphous glycine/water glass phase (i.e., frozen solution) at *ca*. 173.9 ppm. No sharp signals characteristic of crystalline polymorphs of glycine were observed. This result confirms that no detectable amounts of crystallization are induced by the rapid quenching step, and therefore we may conclude that crystalline phases observed in the experiments discussed below are produced during the crystallization process at ambient temperature prior to the rapid quenching step.

First, we consider crystallization from an aqueous solution containing 1-^{13}C-glycine (6 M) and the DNP polarizing agent AMUPol[43] (0.02 M), using water at natural isotopic abundance (H_2O). Three different samples were extracted from the crystallization solution and investigated using the

experimental strategy described above (for more details of the experimental procedure, see Section 2.2 in SI).

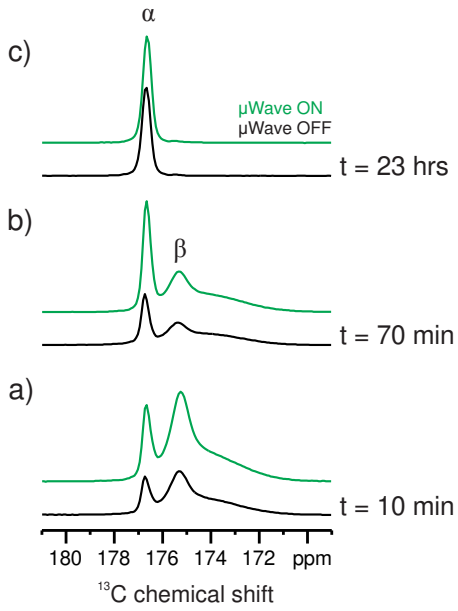

Figure 2. $^{1}H \rightarrow ^{13}C$ CPMAS NMR spectra recorded with (green spectra) and without (black spectra) microwave irradiation for rapidly quenched crystallization solutions containing 1-^{13}C-glycine and AMUPol in H_2O. The three samples were flash cooled to *ca*. 100 K after crystallization times of (a) 10 min, (b) 70 min, (c) 23 hr. The time to record each spectrum was 6 min.

Figure 2 shows $^{1}H \rightarrow ^{13}C$ CPMAS NMR spectra recorded for the three samples of the crystallization solution quenched at different times. The spectrum (Figure 2a) of the sample quenched at 10 min after the start of crystallization has signals characteristic of the α polymorph (176.8 ppm) and β polymorph (175.5 ppm) of glycine. [At 100 K, the isotropic ^{13}C chemical shifts for the carboxylate carbon environment in the α, β and γ polymorphs are 176.8, 175.5 and 174.3 ppm respectively]. [42] In addition, a broad signal corresponding to the amorphous glycine/water glass phase is observed at *ca*. 173.9 ppm. The spectrum (Figure 2b) of the sample quenched at 70 min also contains signals due to the α and β polymorphs, but with increased intensity for the α polymorph and decreased intensity for both the glycine/water glass phase and the β polymorph. These observations indicate that the overall changes occurring between 10 min and 70 min were the transformation of the β polymorph to the α polymorph and the occurrence of further crystallization (either to produce the α polymorph directly

or to produce the β polymorph initially followed by transformation to the α polymorph). The spectrum (Figure 2c) of the sample quenched at 23 hr contains a strong signal only for the α polymorph, and any remaining signals for the β polymorph and the glycine/water glass phase are barely detectable.

These results are consistent with previous literature[37, 44] on crystallization of glycine from natural-isotopic-abundance water, for which the α polymorph is the expected product after a period of *ca*. 1 day. The fact that the same behavior is observed in our solid-state DNP NMR results suggests that the specific conditions of our experiments (including the presence of the DNP polarizing agent in the crystallization solution) do not alter, at least qualitatively, the outcome of the crystallization process. Significantly, the transient intermediate β polymorph was successfully "trapped" in the snapshots of the crystallization process at 10 min and 70 min. We emphasize that this meta-stable polymorph would survive for a significant time if maintained at the quench temperature (*ca*. 100 K), allowing a range of more detailed DNP NMR measurements to be carried out (see below) on the quenched solution containing this polymorph.

In Figures 2a,b, the $^{1}H \rightarrow ^{13}C$ CPMAS NMR spectra recorded with microwave irradiation correspond to DNP signal enhancements of $\varepsilon_{DNP} \approx 2$ relative to the spectra recorded on the same sample without microwave irradiation, but no DNP signal enhancement ($\varepsilon_{DNP} \approx 1$) is observed for the spectrum shown in Figure 2c. These relatively low DNP enhancements may be a consequence of a non-homogeneous distribution of polarizing agent within the glycine/water glass phase, with a deficit of polarizing agent in the close vicinity of the crystalline particles.[45-48]

In an attempt to increase the DNP enhancement, the experiment was repeated with glycerol added to the crystallization solution (see Section 2.3 of SI), as it is known[45, 46] that DNP enhancement in aqueous solutions can be increased in the presence of glycerol (up to 60%). In the present work, however, the amount of glycerol was kept relatively low to minimize the risk that it may affect the crystallization process (we note that nucleation of glycine is reported to be unaffected by small amounts of impurities or additives,[49, 50] although they may have an effect on the kinetics of the

appearance/disappearance of different polymorphs during crystallization[51, 52]). Our experiments (Figure 3) on a solution of 1-^{13}C-glycine and AMUPol dissolved in water/glycerol (95/5 ratio by volume) gave similar results to those observed for crystallization in the absence of glycerol (Figure 2). Thus, both the α and β polymorphs are present in the earliest snapshot of the crystallization process (Figure 3a; deconvolution of the different signals is shown in Figure S2), followed by a decrease in the β polymorph and an increase in the α polymorph as a function of time (Figure 3b), and essentially only the α polymorph is present after a crystallization time of 24 hr (Figure 3c). These results confirm that, in qualitative terms, the pathway of the crystallization process is not modified by the presence of glycerol.

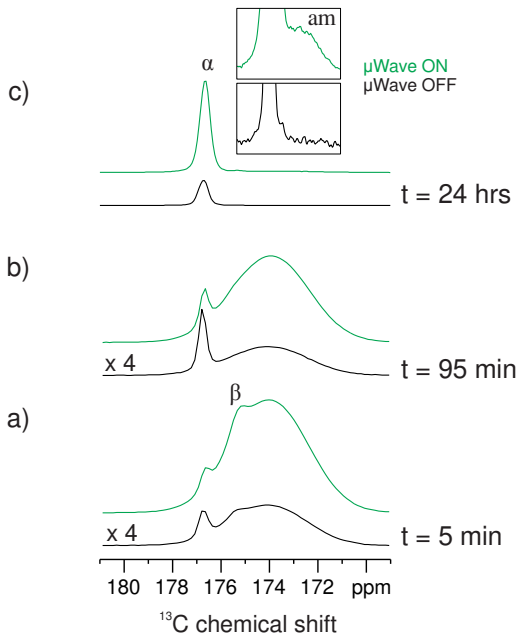

Figure 3. ^{1}H→^{13}C CPMAS NMR spectra recorded with (green spectra) and without (black spectra) microwave irradiation for rapidly quenched crystallization solutions containing 1-^{13}C-glycine and AMUPol in H_2O/glycerol. The three samples were flash cooled to *ca*. 100 K after crystallization times of (a) 5 min, (b) 95 min, (c) 24 hr. The time to record each spectrum was 6 min.

The presence of glycerol gives rise to greater DNP signal enhancements than those for the pure aqueous solution, with $\varepsilon_{DNP} \approx 4$ for the α polymorph and $\varepsilon_{DNP} \approx 13$ for both the β polymorph and the glycine/water glass phase. We note that the increased DNP sensitivity allows a residual amount of

glycine in the glycine/water glass phase to be detected in the sample quenched at 24 hr (see inset in Figure 3c).

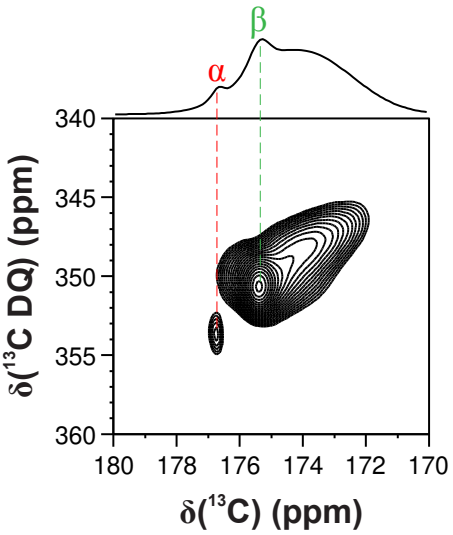

Figure 4. DNP-enhanced ^{13}C-^{13}C DQ dipolar correlation spectrum recorded (recoupling time, 2 ms) for a rapidly quenched crystallization solution containing 1-^{13}C-glycine and AMUPol in water/glycerol. The crystallization time before quenching was 5 min.

This DNP sensitivity enhancement has been exploited to investigate the intermolecular interactions in the glycine/water glass phase in more detail by measuring the 2D DNP-enhanced ^{13}C-^{13}C double-quantum (DQ) dipolar correlation spectrum (Figure 4) for the water/glycerol crystallization solution quenched at 5 min. As 1-^{13}C-glycine was used, correlation peaks in the 2D ^{13}C-^{13}C DQ dipolar correlation spectrum arise only for $^{13}C\cdots{}^{13}C$ intermolecular distances between ^{13}C nuclei in the carboxylate groups of different glycine molecules. Furthermore, as this spectrum was recorded with a relatively short recoupling time (2 ms), we estimate that a correlation signal is observed when the distance between two ^{13}C nuclei is less than 5 Å.[53, 54] In Figure 4, auto-correlation signals arise mainly from the shortest intermolecular $^{13}C\cdots{}^{13}C$ distances between carboxylate groups in the α and β polymorphs (3.09 Å and 3.34 Å, respectively) and also in the glycine/water glass phase, suggesting that at least some short intermolecular glycine-glycine distances exist within the glycine/water glass phase (and hence in the crystallization solution prior to quenching). These short glycine-glycine distances within the glycine/water glass phase could possibly represent pre-nucleation clusters present in the super-saturated crystallization solution prior to quenching, although more detailed studies

(including the use of other experimental and computational techniques) would be required to verify this possible interpretation.

Finally, crystallization from a solution of 1-^{13}C-glycine (6 M) and AMUPol (0.02 M) in deuterated water (D_2O) was also studied (see Section 2.5 of SI). As discussed above, crystallization of glycine from deuterated water over a period of *ca*. 1 day is expected to yield the γ polymorph. The $^{1}H \rightarrow ^{13}C$ CPMAS NMR spectrum recorded on quenching the crystallization solution after 5 min (Figure S3a) contains signals due to the α, β and γ polymorphs. After 60 min (Figure S3b), there is no signal due to the β polymorph, while the intensities of the signals for the α and γ polymorphs have increased. At 23 hr (Figure S3c), the signal due to the γ polymorph has further increased significantly, while the signal for the α polymorph has diminished. These results are clearly in full agreement with earlier literature[4, 8, 35, 39] which showed that formation of the thermodynamically stable γ polymorph is accelerated in crystallization of glycine from D_2O compared to H_2O (compare the results in Figure S3 and Figure 2, respectively).

In conclusion, we have demonstrated that low-temperature solid-state NMR measurements, with DNP enhancement, represent a promising *ex-situ* method for studying the consecutive stages of crystallization processes, including the opportunity to measure sophisticated 2D NMR spectra for quenched samples of the crystallization system preserved at the quench temperature. Our results demonstrate that specific requirements of the experimental procedure (e.g., the presence of the DNP polarizing agent in the crystallization solution and/or the addition of glycerol) do not modify the sequence of solid forms present during the crystallization process, although we cannot rule out the possibility that the presence of a DNP polarizing agent or other additives within the crystallization solution might modify the details of the crystallization pathway under some circumstances. Furthermore, the use of DNP methodology can dramatically increase the sensitivity of the NMR measurements (by a factor of up to 13 in the present work), which is advantageous in allowing a range of solid-state NMR methods to be applied for detailed structural characterization of transient solid

forms. The strategy reported here is complementary to existing solid-state NMR methods for studying crystallization processes, but crucially the opportunity to exploit DNP sensitivity enhancement opens up the prospect of gaining insights into much earlier stages of crystallization than has been possible hitherto, as the amount of the solid phases present at the very early stages of crystallization is intrinsically low.

ASSOCIATED CONTENT

Supporting Information.

Supporting Information is available free of charge. Experimental details, deconvolution of the spectra shown in Figure 3a, and results of experiments involving flash cooling of dilute aqueous solutions of glycine and experiments involving crystallization of glycine from D_2O (PDF).

AUTHOR INFORMATION

The authors declare no competing financial interests.

ACKNOWLEDGMENT

We thank Bruker SAS for access to the solid-state NMR spectrometer used here and Dr F. Aussenac and Dr P. Dorffer for experimental assistance. This project received funding from the European Research Council (ERC) under the European Union Horizon 2020 research and innovation programme (grant agreement No. 758498). Preliminary results were obtained thanks to the support of Agence Nationale de la Recherche (grant number ANR-13-JS080001). Cardiff University is also thanked for support.

REFERENCES

1. Van Driessche, A. E. S.; Van Gerven, N.; Bomans, P. H. H.; Joosten, R. R. M.; Friedrich, H.; Gil-Carton, D.; Sommerdijk, N. A. J. M.; Sleutel, M., Molecular Nucleation Mechanisms and Control Strategies for Crystal Polymorph Selection. *Nature* **2018,** *556*, 89.

2. Desiraju, G. R., Crystal Engineering: From Molecule to Crystal. *J. Am. Chem. Soc.* **2013,** *135*, 9952-9967.

3. Cruz-Cabeza, A. J.; Reutzel-Edens, S. M.; Bernstein, J., Facts and Fictions about Polymorphism. *Chem. Soc. Rev.* **2015,** *44*, 8619-8635.

4. Hughes, C. E.; Hamad, S.; Harris, K. D. M.; Catlow, C. R. A.; Griffiths, P. C., A Multi-technique Approach for Probing the Evolution of Structural Properties during Crystallization of Organic Materials from Solution. *Faraday Discuss.* **2007,** *136*, 71-89.

5. Nicole, P.; Wolfgang, B., In- Situ Monitoring of the Formation of Crystalline Solids. *Angew. Chem. Int. Ed.* **2011,** *50*, 2014-2034.

6. Schreiber, R. E.; Houben, L.; Wolf, S. G.; Leitus, G.; Lang, Z.-L.; Carbó, J. J.; Poblet, J. M.; Neumann, R., Real-time Molecular Scale Observation of Crystal Formation. *Nat. Chem.* **2016,** *9*, 369.

7. Senker, J.; Sehnert, J.; Correll, S., Microscopic Description of the Polyamorphic Phases of Triphenyl Phosphite by Means of Multidimensional Solid-State NMR Spectroscopy. *J. Am. Chem. Soc.* **2005,** *127*, 337-349.

8. Hughes, C. E.; Harris, K. D. M., A Technique for In Situ Monitoring of Crystallization from Solution by Solid-State ^{13}C CPMAS NMR Spectroscopy. *J. Phys. Chem. A* **2008,** *112*, 6808-6810.

9. Hughes, C. E.; Harris, K. D. M., Direct Observation of a Transient Polymorph during Crystallization. *Chem. Commun.* **2010,** *46*, 4982-4984.

10. Hughes, C. E.; Williams, P. A.; Peskett, T. R.; Harris, K. D. M., Exploiting In Situ Solid-State NMR for the Discovery of New Polymorphs during Crystallization Processes. *J. Phys. Chem. Lett.* **2012,** *3*, 3176-3181.

11. Hughes, C. E.; Williams, P. A.; Harris, K. D. M., "CLASSIC NMR": An In-Situ NMR Strategy for Mapping the Time-Evolution of Crystallization Processes by Combined Liquid-State and Solid-State Measurements. *Angew. Chem. Int. Ed.* **2014,** *53*, 8939-8943.

12. Radhakrishnan, S.; Goossens, P. J.; Magusin, P. C.; Sree, S. P.; Detavernier, C.; Breynaert, E.; Martineau, C.; Taulelle, F.; Martens, J. A., In Situ Solid-State ^{13}C NMR Observation of Pore Mouth Catalysis in Etherification of β-Citronellene with Ethanol on Zeolite Beta. *J. Am. Chem. Soc.* **2016,** *138*, 2802-2808.

13. Ivanova, I. I.; Kolyagin, Y. G.; Kasyanov, I. A.; Yakimov, A. V.; Bok, T. O.; Zarubin, D. N., Time-Resolved In-Situ MAS NMR Monitoring of the Nucleation and Growth of Zeolite BEA Catalysts under Hydrothermal Conditions. *Angew. Chem. Int. Ed.* **2017,** *56*, 15344-15347.

14. Hughes, C. E.; Williams, P. A.; Kariuki, B. M.; Harris, K. D. M., Establishing the Transitory Existence of Amorphous Phases in Crystallization Pathways by the CLASSIC NMR Technique. *ChemPhysChem* **2018,** *19*, 3341-3345.

15. Concistrè, M.; Gansmüller, A.; McLean, N.; Johannessen, O. G.; Marín Montesinos, I.; Bovee-Geurts, P. H. M.; Brown, R. C. D.; DeGrip, W. J.; Levitt, M. H., Light Penetration and Photoisomerization in Rhodopsin studied by Numerical Simulations and Double-Quantum Solid-State NMR Spectroscopy. *J. Am. Chem. Soc.* **2009,** *131*, 6133-6140.

16. Lipton, A. S.; Heck, R. W.; de Jong, W. A.; Gao, A. R.; Wu, X.; Roehrich, A.; Harbison, G. S.; Ellis, P. D., Low Temperature ^{65}Cu NMR Spectroscopy of the Cu^{+} Site in Azurin. *J. Am. Chem. Soc.* **2009,** *131*, 13992-13999.

17. Hu, K.-N.; Yau, W.-M.; Tycko, R., Detection of a Transient Intermediate in a Rapid Protein Folding Process by Solid-State Nuclear Magnetic Resonance. *J. Am. Chem. Soc.* **2010,** *132*, 24-25.

18. Concistrè, M.; Carignani, E.; Borsacchi, S.; Johannessen, O. G.; Mennucci, B.; Yang, Y.; Geppi, M.; Levitt, M. H., Freezing of Molecular Motions Probed by Cryogenic Magic Angle Spinning NMR. *J. Phys. Chem. Lett.* **2014,** *5*, 512-516.

19. Ni, Q. Z.; Daviso, E.; Can, T. V.; Markhasin, E.; Jawla, S. K.; Swager, T. M.; Temkin, R. J.; Herzfeld, J.; Griffin, R. G., High Frequency Dynamic Nuclear Polarization. *Acc. Chem. Res.* **2013,** *46*, 1933-1941.

20. Rossini, A. J.; Zagdoun, A.; Lelli, M.; Lesage, A.; Copéret, C.; Emsley, L., Dynamic Nuclear Polarization Surface Enhanced NMR Spectroscopy. *Acc. Chem. Res.* **2013,** *46*, 1942-1951.

21. Smith, A. N.; Long, J. R., Dynamic Nuclear Polarization as an Enabling Technology for Solid State Nuclear Magnetic Resonance Spectroscopy. *Anal. Chem.* **2016,** *88*, 122-132.

22. Potapov, A.; Yau, W.-M.; Ghirlando, R.; Thurber, K. R.; Tycko, R., Successive Stages of Amyloid-β Self-Assembly Characterized by Solid-State Nuclear Magnetic Resonance with Dynamic Nuclear Polarization. *J. Am. Chem. Soc.* **2015,** *137*, 8294-8307.

23. Kobayashi, T.; Perras, F. A.; Goh, T. W.; Metz, T. L.; Huang, W.; Pruski, M., DNP-Enhanced Ultrawideline Solid-State NMR Spectroscopy: Studies of Platinum in Metal–Organic Frameworks. *J. Phys. Chem. Lett.* **2016,** *7*, 2322-2327.

24. Lee, D.; Hediger, S.; Paëpe, G. D., High-Field Solid-State NMR with Dynamic Nuclear Polarization. In *Modern Magnetic Resonance*, Webb, G. A., Ed. Springer International Publishing: 2017; pp 1-17.

25. Lilly Thankamony, A. S.; Wittmann, J. J.; Kaushik, M.; Corzilius, B., Dynamic Nuclear Polarization for Sensitivity Enhancement in Modern Solid-state NMR. *Prog. Nucl. Magn. Reson. Spectros.* **2017,** *102-103*, 120-195.

26. Plainchont, B.; Berruyer, P.; Dumez, J.-N.; Jannin, S.; Giraudeau, P., Dynamic Nuclear Polarization Opens New Perspectives for NMR Spectroscopy in Analytical Chemistry. *Anal. Chem.* **2018,** *90*, 3639-3650.

27. Rossini, A. J., Materials Characterization by Dynamic Nuclear Polarization-Enhanced Solid-State NMR Spectroscopy. *J. Phys. Chem. Lett.* **2018,** *9*, 5150-5159.

28. Saliba, E. P.; Sesti, E. L.; Alaniva, N.; Barnes, A. B., Pulsed Electron Decoupling and Strategies for Time Domain Dynamic Nuclear Polarization with Magic Angle Spinning. *J. Phys. Chem. Lett.* **2018,** *9*, 5539-5547.

29. Lilly-Thankamony, A. S.; Lion, C.; Pourpoint, F.; Singh, B.; Perez-Linde, A. J.; Carnevale, D.; Bodenhausen, G.; Vezin, H.; Lafon, O.; Polshettiwar, V., Insights into the Catalytic Activity of Nitridated Fibrous Silica (KCC-1) Nanocatalysts from ^{15}N and ^{29}Si NMR Spectroscopy Enhanced by Dynamic Nuclear Polarization. *Angew. Chem. Int. Ed.* **2015,** *54*, 2190-2193.

30. Bothe, S.; Nowag, J.; Klimavičius, V.; Hoffmann, M.; Troitskaya, T. I.; Amosov, E. V.; Tormyshev, V. M.; Kirilyuk, I.; Taratayko, A.; Kuzhelev, A.; Parkhomenko, D.; Bagryanskaya, E.; Gutmann, T.; Buntkowsky, G., Novel Biradicals for Direct Excitation Highfield Dynamic Nuclear Polarization. *J. Phys. Chem. C* **2018,** *122*, 11422-11432.

31. Equbal, A.; Li, Y.; Leavesley, A.; Huang, S.; Rajca, S.; Rajca, A.; Han, S., Truncated Cross Effect Dynamic Nuclear Polarization: An Overhauser Effect Doppelgänger. *J. Phys. Chem. Lett.* **2018,** *9*, 2175-2180.

32. Sani, M.-A.; Martin, P.-A.; Yunis, R.; Chen, F.; Forsyth, M.; Deschamps, M.; O'Dell, L. A., Probing Ionic Liquid Electrolyte Structure via the Glassy State by Dynamic Nuclear Polarization NMR Spectroscopy. *J. Phys. Chem. Lett.* **2018,** *9*, 1007-1011.

33. Albrecht, G.; Corey, R. B., The Crystal Structure of Glycine. *J. Am. Chem. Soc.* **1939,** *61*, 1087-1103.

34. Iitaka, Y., The Crystal Structure of β-Glycine. *Acta Crystallogr.* **1960,** *13*, 35-45.

35. Iitaka, Y., The Crystal Structure of γ-Glycine. *Acta Crystallogr.* **1961,** *14*, 1-10.

36. Jonsson, P. G.; Kvick, A., Precision Neutron Diffraction Structure Determination of Protein and Nucleic Acid Components. III. The Crystal and Molecular Structure of the Amino Acid α-Glycine. *Acta Crystallogr. B* **1972,** *28*, 1827-1833.

37. Boldyreva, E. V.; Drebushchak, V. A.; Drebushchak, T. N.; Paukov, I. E.; Kovalevskaya, Y. A.; Shutova, E. S., Polymorphism of Glycine, Part I. *J. Therm. Anal. Calorim.* **2003,** *73*, 409-418.

38. Perlovich, G. L.; Hansen, L. K.; Bauer-Brandl, A., The Polymorphism of Glycine. Thermochemical and Structural Aspects. *J. Therm. Anal. Calorim.* **2001,** *66*, 699-715.

39. Hughes, C. E.; Harris, K. D. M., The eEfect of Deuteration on Polymorphic Outcome in the Crystallization of Glycine from Aqueous Solution. *New J. Chem.* **2009,** *33*, 713-716.

40. Taylor, R. E., ^{13}C CP/MAS: Application to Glycine. *Concepts Magn. Reson.* **2004,** *22A*, 79-89.

41. Xu, W.; Zhu, Q.; Hu, C., The Structure of Glycine Dihydrate: Implications for the Crystallization of Glycine from Solution and Its Structure in Outer Space. *Angew. Chem. Int. Ed.* **2017,** *56*, 2030-2034.

42. Cerreia Vioglio, P.; Mollica, G.; Juramy, M.; Hughes, C. E.; Williams, P. A.; Ziarelli, F.; Viel, S.; Thureau, P.; Harris, K. D. M., Insights into the Crystallization and Structural Evolution of Glycine Dihydrate by In-Situ Solid-State NMR Spectroscopy. *Angew. Chem. Int. Ed.* **2018,** *57*, 6619-6623.

43. Sauvée, C.; Rosay, M.; Casano, G.; Aussenac, F.; Weber, R. T.; Ouari, O.; Tordo, P., Highly Efficient, Water-Soluble Polarizing Agents for Dynamic Nuclear Polarization at High Frequency. *Angew. Chem. Int. Ed.* **2013,** *52*, 10858-10861.

44. Towler, C. S.; Davey, R. J.; Lancaster, R. W.; Price, C. J., Impact of Molecular Speciation on Crystal Nucleation in Polymorphic Systems: The Conundrum of γ Glycine and Molecular 'Self Poisoning'. *J. Am. Chem. Soc.* **2004,** *126*, 13347-13353.

45. Gerfen, G. J.; Becerra, L. R.; Hall, D. A.; Griffin, R. G.; Temkin, R. J.; Singel, D. J., High Frequency (140 GHz) Dynamic Nuclear Polarization: Polarization Transfer to a Solute in Frozen Aqueous Solution. *J. Chem. Phys.* **1995,** *102*, 9494-9497.

46. Hall, D. A.; Maus, D. C.; Gerfen, G. J.; Inati, S. J.; Becerra, L. R.; Dahlquist, F. W.; Griffin, R. G., Polarization-Enhanced NMR Spectroscopy of Biomolecules in Frozen Solution. *Science* **1997,** *276*, 930.

47. Kiesewetter, M. K.; Corzilius, B.; Smith, A. A.; Griffin, R. G.; Swager, T. M., Dynamic Nuclear Polarization with a Water-Soluble Rigid Biradical. *J. Am. Chem. Soc.* **2012,** *134*, 4537-4540.

48. Takahashi, H.; Fernández-de-Alba, C.; Lee, D.; Maurel, V.; Gambarelli, S.; Bardet, M.; Hediger, S.; Barra, A.-L.; De Paëpe, G., Optimization of an Absolute Sensitivity in a Glassy Matrix during DNP-enhanced Multidimensional Solid-state NMR Experiments. *J. Magn. Reson.* **2014,** *239*, 91-99.

49. Davey, R. J.; Schroeder, S. L. M.; ter Horst, J. H., Nucleation of Organic Crystals—A Molecular Perspective. *Angew. Chem. Int. Ed.* **2013,** *52*, 2166-2179.

50. Meirzadeh, E.; Dishon, S.; Weissbuch, I.; Ehre, D.; Lahav, M.; Lubomirsky, I., Solvent-Induced Crystal Polymorphism as Studied by Pyroelectric Measurements and Impedance Spectroscopy: Alcohols as Tailor-Made Inhibitors of α-Glycine. *Angew. Chem. Int. Ed.* **2018,** *57*, 4965-4969.

51. Weissbuch, I.; Torbeev, V. Y.; Leiserowitz, L.; Lahav, M., Solvent Effect on Crystal Polymorphism: Why Addition of Methanol or Ethanol to Aqueous Solutions Induces the Precipitation of the Least Stable β Form of Glycine. *Angew. Chem. Int. Ed.* **2005,** *44*, 3226-3229.

52. Dowling, R.; Davey, R. J.; Curtis, R. A.; Han, G.; Poornachary, S. K.; Chow, P. S.; Tan, R. B. H., Acceleration of Crystal Growth Rates: an Unexpected Effect of Tailor-made Additives. *Chem. Commun.* **2010,** *46*, 5924-5926.

53. Takahashi, H.; Lee, D.; Dubois, L.; Bardet, M.; Hediger, S.; De Paëpe, G., Rapid Natural-Abundance 2D ^{13}C–^{13}C Correlation Spectroscopy Using Dynamic Nuclear Polarization Enhanced Solid-State NMR and Matrix-Free Sample Preparation. *Angew. Chem. Int. Ed.* **2012,** *51*, 11766-11769.

54. Mollica, G.; Dekhil, M.; Ziarelli, F.; Thureau, P.; Viel, S., Quantitative Structural Constraints for Organic Powders at Natural Isotopic Abundance Using Dynamic Nuclear Polarization Solid-State NMR Spectroscopy. *Angew. Chem. Int. Ed.* **2015,** *54*, 6028-6031.